ELSEVIER

Journal of Alloys and Compounds 275–277 (1998) 911–914

Journal of ALLOYS AND COMPOUNDS

Y(III)-enhanced Dy(III) and Sm(III)-specific electrogenerated luminescence of heterodinuclear **1**–Y(III)–Dy(III)–**1** and **1**–Y(III)–Sm(III)–**1** chelates

Timo Ala-Kleme*, Keijo Haapakka, Martti Latva

Department of Chemistry, University of Turku, FIN-20014 Turku, Finland

Abstract

1 is a heptadentate chelating agent which forms stable dimer-like dinuclear chelates. At a pulse-polarized oxide-covered aluminium cathode in the presence of peroxydisulfate, the homodinuclear **1**–Y(III)–Y(III)–**1** chelate generates a weak Y(III)-initiated ligand-centered 322 nm ECL, while the homodinuclear **1**–Ln(III)′–Ln(III)′–**1** and heterodinuclear **1**–Y(III)–Ln(III)′–**1** chelates (Ln(III)′=Dy(III), Sm(III)) initiate intense ligand-sensitized Dy(III)-specific and Sm(III)-specific $^4F_{9/2}\rightarrow{}^6H_j$ and $^4G_{5/2}\rightarrow{}^6H_j$ transitions, respectively, so that the ECL efficiency of the heterodinuclear chelate is around ten-fold as compared with that of the corresponding homodinuclear chelate. © 1998 Elsevier Science S.A.

Keywords: Chelating agents; Electrochemiluminescence

1. Introduction

2,6-Bis[*N*,*N*-bis(carboxymethyl)aminomethyl]-4-benzoylphenol (**1**) is a heptadentate chelating agent which is capable of forming self-assembled dimer-like homodinuclear **1**–Ln(III)–Ln(III)–**1** and heterodinuclear **1**–Ln(III)–Ln(III)′–**1** chelates in aqueous solutions [1,2]. Depending on the energy levels of their excited states, the homodinuclear Ln(III)/Ln(III) and heterodinuclear Ln(III)/Ln(III)′ edifices may be either single or double nuclear intramolecular relaxation centers for the triplet energy T_1 of **1**, finally initiating the ligand-sensitized radiative lanthanide(III)-specific transitions, providing that at least one of the lanthanide(III) cations belongs to the group Dy(III), Eu(III), Sm(III), Tb(III). In addition, our luminescence studies have pointed out that the relative luminescence yield of the ligand-sensitized radiative $^5D_0\rightarrow{}^7F_j$ transitions of Eu(III) is higher by a factor of approximately 2 in the heterodinuclear **1**–Y(III)–Eu(III)–**1** chelate than in the homodinuclear **1**–Eu(III)–Eu(III)–**1** chelate, which could be assigned to the increased energy donor–acceptor ratio [2].

This contribution deals with the Y(III)-initiated ligand-centered electrochemiluminescence (ECL) and ligand-sensitized Ln(III)′-specific ECL at the pulse-polarized oxide-covered aluminium cathode generated in sample mixtures containing homodinuclear **1**–Y(III)–Y(III)–**1**, **1**–Ln(III)′–Ln(III)′–**1** and heterodinuclear **1**–Y(III)–Ln(III)′–**1** chelates (Ln(III)′=Dy(III), Sm(III)) and peroxydisulfate, and demonstrates that the relaxation of the electrochemically generated ligand-centered T_1 state to the Y(III)/Ln(III)′ single nuclear edifice to induce the radiative Dy(III)-specific and Sm(III)-specific $^4F_{9/2}\rightarrow{}^6H_j$ and $^4G_{5/2}\rightarrow{}^6H_j$ transition, respectively, is drastically higher than that of the Ln(III)′/Ln(III)′ double nuclear edifice.

2. Experimental

2.1. Instrumentation

A Perkin-Elmer LS-5 luminescence spectrometer was used to measure the ECL spectra where an oxide-covered Al-sheet working electrode and a Pt wire counter electrode were placed in a conventional quartz cuvette: the surface area and oxide layer thickness of the working electrode were $A\approx0.8\ cm^2$ and $d\approx4$ nm. The ECL measurements were conducted using a potentiostatic pulse generator with 0.2 ms and 10.0 V cathodic excitation pulses with a 10 ms intermittent zero level; the cathodic current density was $j\approx80\ mA\ cm^{-2}$ in the sample solutions.

2.2. Reagents

Dysprosium(III) oxide (Aldrich), samarium(III) nitrate (Alfa), yttrium(III) oxide (Aldrich), potassium peroxydisul-

*Corresponding author.

0925-8388/98/$19.00
PII: S0925-8388(98)00483-6

Table 1
Relative amounts of homodinuclear **1**–Y(III)–Y(III)–**1**, **1**–Ln(III)′–Ln(III)′–**1** and heterodinuclear **1**–Y(III)–Ln(III)′–**1** chelates; the solutions are 1.00×10^{-5} M with respect to **1**

Mixture	[Y(III)+Ln(III)′] (10^{-6} M)	**1**--Y(III)–Y(III)–**1** (%)	**1**–Ln(III)′–Ln(III)′–**1** (%)	**1**–Y(III)–Ln(III)′–**1** (%)
I	10.0+0	100	0	0
II	9.0+1.0	81	1	18
III	7.0+3.0	49	9	42
IV	5.0+5.0	25	25	50
V	3.0+7.0	9	49	42
VI	1.0+9.0	1	81	18

fate (Merck) and sodium tetraborate decahydrate (Merck) were used as received. **1** was synthesized as described elsewhere [3]. The 1.00×10^{-2} M stock solutions of Dy(III) and Y(III) were prepared in perchloric acid and that of Sm(III) in water. Quartz-distilled water was used for the preparation of all solutions.

The sample solutions containing the homodinuclear **1**–Y(III)–Y(III)–**1** and **1**–Ln(III)′–Ln(III)′–**1** and heterodinuclear **1**–Y(III)–Ln(III)′–**1** chelates were obtained by diluting an appropriate mixture of Y(III) and Ln(III)′ in an equimolar solution of **1** adjusted to pH 9.2 by borate buffer; these sample solutions were then allowed to equilibrate overnight at ambient temperature before the ECL measurement. Table 1 lists the statistically expected amounts of these dinuclear chelates under the different mixing conditions.

3. Results and discussion

3.1. Self-assembled dimer-like dinuclear lanthanide(III) chelates

1 is a heptadentate chelating agent furnished with one phenolic hydroxyl group and two flexible 2,2′-(methylenenitrilo)bis(acetic acid) moieties to form thermodynamically and kinetically stable, self-assembled dimer-like lanthanide(III) chelates in aqueous solutions as displayed schematically in Fig. 1, where the chelating cage locates two lanthanide(III) cations coordinated by two nitrogen and two oxygen ligand atoms and, in addition, by the deprotonated hydroxyl group of both ligands **1** [1].

The Y(III) cation and the Dy(III) and Sm(III) cations denoted subsequently as Ln(III)′ form structurally similar dinuclear chelates, mainly because of their essentially spherical geometry in association with large and relatively similar ionic radii. On this basis, Table 1 lists the mixtures of homodinuclear **1**–Y(III)–Y(III)–**1** and **1**–Ln(III)′–Ln(III)′–**1** and heterodinuclear **1**–Y(III)–Ln(III)′–**1** chelates with their statistically estimated amounts formed in the sample solutions, where the concentration of **1** and the total concentration of Y(III) and Ln(III)′ are strictly equimolar [1,2].

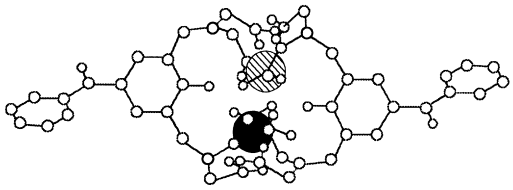

Fig. 1. Schematic diagram of the structure of the dinuclear lanthanide(III) chelate: homodinuclear chelate **1**–Ln(III)–Ln(III)–**1**, heterodinuclear chelate **1**–Ln(III)–Ln(III)′–**1**.

3.2. Cathodic Y(III)-initiated ligand-centered and Y(III)-enhanced Ln(III)′-specific ECL of the dinuclear chelates

Cathodic pulse-polarization of the oxide-covered aluminium electrode in the presence of peroxydisulfate initiates a 420 nm F-center emission at the electrode/electrolyte interface where the cathodically generated hydrated electron e^-_{aq} and sulfate monoanion radical SO_4^- play a role of vital importance [4] (Fig. 2). These intermediates provide the basis for the luminophore-specific cathodic ECLs by the Ox/Red excitation mechanism [5].

Figs. 3 and 4 display the ECL spectra measured from the cathodically pulse-polarized electrode/electrolyte interface in the presence of the stated concentrations of potassium peroxydisulfate, **1**–Y(III)–Y(III)–**1**, **1**–Ln(III)′–Ln(III)′–**1** and **1**–Y(III)–Ln(III)′–**1** (i.e., sample mixtures

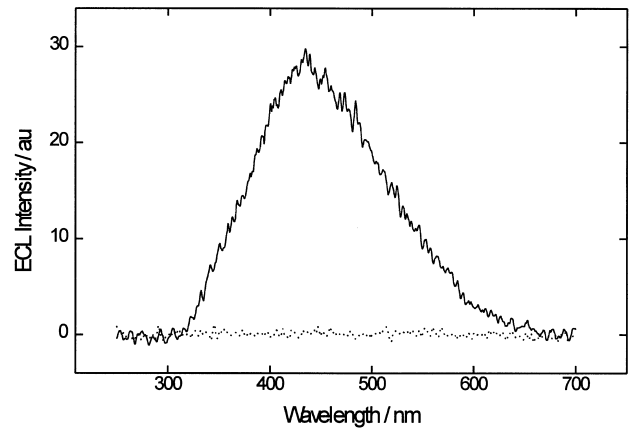

Fig. 2. F-center ECL of the pulse-polarized oxide-covered aluminium cathode: (· · ·) without and (———) with potassium peroxydisulfate. Conditions: generation of ECL, see Experimental; electrolyte, 5.0×10^{-2} M $Na_2B_4O_7$ at pH 9.2 containing 3.0×10^{-3} M $Na_2S_2O_8$.

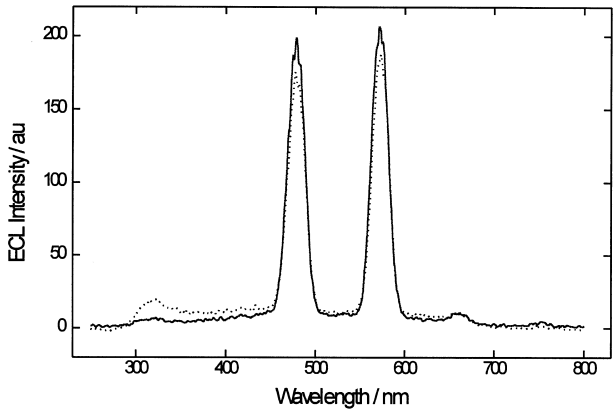

Fig. 3. Cathodic Dy(III)-specific ECL: (· · ·) sample mixture III and (———) sample mixture V of Table 1. Conditions: generation of ECL and electrolyte, as in Fig. 2.

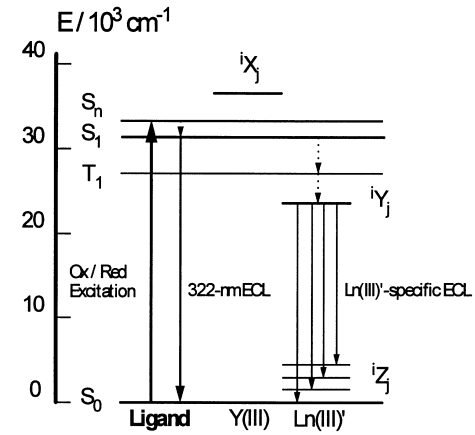

Fig. 5. Schematic diagram of the energy flow in the dinuclear chelates (see text for details).

III and V of Table 1). These results can be interpreted as follows: (i) the ECL spectra contain a common broad emission band at $\lambda = 322$ nm; this band can be assigned to a Y(III)-initiated ligand-centered $S_1 \rightarrow S_0$ transition, but occurs only in the homodinuclear **1**–Y(III)–Y(III)–**1** chelate; (ii) the narrow emission bands at $\lambda = 483$, 585 and 666 nm (Fig. 3) and $\lambda = 562$, 597, 645 and 707 nm (Fig. 4) can be assigned to the well-known $^4F_{9/2} \rightarrow {}^6H_{15/2 \rightarrow 11/2}$ and $^4G_{5/2} \rightarrow {}^6H_{5/2 \rightarrow 11/2}$ transitions of Dy(III) and Sm(III), respectively [6], and denoted subsequently as the cathodic Dy(III)-specific and Sm(III)-specific ECLs; and (iii) the intensities of the Dy(III)-specific and Sm(III)-specific ECLs measured from sample mixtures III and V are nearly equal despite their five-fold difference in [**1**–Ln(III)′–Ln(III)′–**1**]; this experimental result shows distinctly that the heterodinuclear **1**–Y(III)–Ln(III)′–**1** chelate is around a 10 times more efficient electroluminophore than the homodinuclear **1**–Ln(III)′–Ln(III)′–**1** chelate.

Fig. 5 displays a generalized energy level diagram to elucidate in more detail the 322 nm ligand-centered, Dy(III)-specific and Sm(III)-specific cathodic ECLs, where

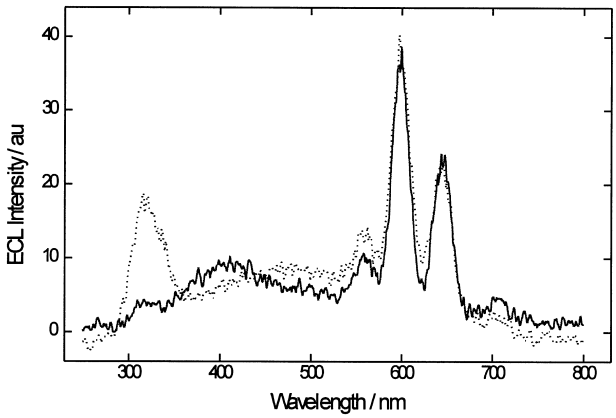

Fig. 4. Cathodic Sm(III)-specific ECL: (· · ·) sample mixture III and (———) sample mixture V of Table 1. Conditions: generation of ECL and electrolyte, as in Fig. 2.

(i) the electrochemical Ox/Red excitation pathway, which involves as a preliminary step the reduction of the carbonyl group of **1**, provides the means to raise the ligand of these dinuclear chelates to their excited singlet level $S_n \approx 33\,000\ cm^{-1}$; the lowest excited singlet $S_1 \approx 31\,000\ cm^{-1}$ and triplet $T_1 \approx 26\,000\ cm^{-1}$ states of the reduced ligand were determined conventionally using 2,6-bis[*N*,*N*-bis(carboxymethyl)aminomethyl]-4-methyl as the photochemical analog of the reduced **1**; (ii) the excited level of Y(III) denoted as ^iX_j is located at an arbitrary level $E \approx 37\,000\ cm^{-1}$ (i.e., Y(III) has no excitation transitions in the range $E = 10\,000–50\,000\ cm^{-1}$ as may be expected from its closed-shell electronic configuration and the absence of unpaired electrons), just to indicate that Y(III) cannot be an acceptor of the excitation energy attained at the cathodically pulse-polarized electrode/electrolyte interface under the present conditions; and, finally, (iii) ^iY_j denotes the excited states of Dy(III) and Sm(III) close to the $T_1 \approx 26\,000\ cm^{-1}$ state of the reduced ligand, and ^iZ_j the vibrational ground state of Dy(III) and Sm(III) as listed in Table 2 [6].

It is postulated that the essential role of Y(III) in the formation of the ligand-centered 322 nm ECL is due to its diamagnetism and its low atomic weight; i.e. these factors decrease the quantum efficiency of the ligand-centered $S_1 \rightarrow T_1$ transition which, in turn, makes the $S_1 \rightarrow S_0$ transition a dominating $S_1 \approx 31\,000\ cm^{-1}$ relaxation pathway to induce the weak 322 nm ECL. In our opinion, the presence of Ln(III)′ inside the chelating cage as the heterocation, changes drastically this ligand-centered $S_1 \approx 31\,000\ cm^{-1}$ relaxation pathway on the following basis: (i) deviating from the diamagnetic Y(III) cation, Ln(III)′ with its high atomic weight is strongly paramagnetic, thus favouring the $S_1 \rightarrow T_1$ transition at the expense of the radiative $S_1 \rightarrow S_0$ transition; and (ii) as listed in Table 2, Ln(III)′ possesses an excited energy level ^iY_j which is very close to that of the T_1 level of the reduced ligand, thus providing a sufficiently small energy gap $\Delta E(T_1 - {}^iY_j)$ for the strong spectral overlap of the energy donor/acceptor couple,

Table 2
Selected excited state energy levels of Ln(III)′ cations between the $T_1 \approx 26\,000\ cm^{-1}$ of the reduced ligand and the lowest excited states $^4F_{9/2} = 21\,057\ cm^{-1}$ of Dy(III) and $^4G_{5/2} = 17\,858\ cm^{-1}$ of Sm(III) depicted as ^iY_j in Fig. 5; ^iZ_j denotes the vibrational ground state levels of Ln(III)′ cations; the energy levels are from Ref. [6]

Ln(III)′	^iY_j (cm^{-1})	^iZ_j (cm^{-1})	λ_{ECL} (nm) (Figs. 3 and 4)
Dy(III)	$^4M_{19/2} = 26\,260$		
	$^4K_{17/2} = 25\,661$		
	$^4M_{21/2} = 24\,990$		
	$^4G_{11/2} = 23\,468$		
	$^4I_{15/2} = 22\,022$		
	$^4F_{9/2} = 21\,057$	$\rightarrow {}^6H_{11/2} = 5882$	659
		$\rightarrow {}^6H_{13/2} = 3502$	570
		$\rightarrow {}^6H_{15/2} = 0$	475
Sm(III)	$^4D_{1/2}$, $^6P_{7/2} = 26\,791$		
	$(^4K,^4L)_{17/2} = 26\,495$		
	$^4K_{11/2} = 25\,166$		
	$^4M_{19/2} = 24\,034$		
	$^4F_{5/2}$, $^4M_{17/2} = 22\,164$		
	$^4I_{13/2} = 21\,663$		
	$^4G_{7/2} = 20\,037$		
	$^4G_{5/2} = 17\,858$	$\rightarrow {}^6H_{11/2} = 3520$	697
		$\rightarrow {}^6H_{9/2} = 2210$	639
		$\rightarrow {}^6H_{7/2} = 1000$	593
		$\rightarrow {}^6H_{5/2} = 0$	560

which is a prerequisite in the $S_1 \approx 31\,000\ cm^{-1}$ relaxation pathway for the radiative Ln(III)′-specific $^iY_j \rightarrow {}^iZ_j$ transitions shown in Figs. 3 and 4.

Perhaps the most interesting result of this study, however, is the experimental finding that the quantum efficiency of the radiative $^iY_j \rightarrow {}^iZ_j$ transition (i.e., the intensity of the Ln(III)′-specific ECL) in the heterodinuclear **1**–Y(III)–Ln(III)′–**1** chelate is around 10 times higher than in the corresponding homodinuclear **1**–Ln(III)′–Ln(III)′–**1** chelate. Much more experimental work is required to treat this Y(III)-enhanced Ln(III)′-specific ECL in detail but, mainly on a qualitative basis, it is tempting to suggest possible ECL enhancement factors specific for the encapsulated heterodinuclear Y(III)/Ln(III)′ edifice as compared to the corresponding homodinuclear Ln(III)′–Ln(III)′ edifices: (i) the ligand-centered Ox/Red excitation pathway may be more efficient; (ii) the energy gaps $\Delta E(S_1 \rightarrow T_1)$ and/or $\Delta E(T_1 \rightarrow {}^iY_j)$ may be more favourable for a stronger spectral overlap of the donor emission and acceptor absorption; (iii) the donor/acceptor distance may be shorter for the intramolecular energy transfer; and, finally, (iv) the high energy level of Y(III) allows the Ln(III)-specific ^iY_j excited state to relax only to the Ln(III)-specific ^iZ_j ground state and, in addition, prevents excitation energy migration between the encapsulated cations inside the chelating cage.

References

[1] M. Latva, S. Kulmala, K. Haapakka, Inorg. Chim. Acta 247 (1996) 209.
[2] M. Latva, P. Mäkinen, S. Kulmala, K. Haapakka, J. Chem. Soc., Faraday Trans. 92(18) (1996) 3321.
[3] J. Kankare, K. Fäldén, S. Kulmala, K. Haapakka, Anal. Chim. Acta 256 (1992) 17.
[4] S. Kulmala, T. Ala-Kleme, A. Hakanen, K. Haapakka, J. Chem. Soc., Faraday Trans. 93(1) (1997) 165.
[5] S. Kulmala, K. Haapakka, J. Alloys Comp. 225 (1995) 502.
[6] C. Morrison, R. Leavitt, in: K. Gschneidner Jr., L. Eyring (Eds.), Handbook on the Physics and Chemistry of Rare Earths, Vol. 5, North-Holland, Amsterdam, 1982, p. 46.